Optica Applicata, Vol. XI, No. 2, 1981

Numerical reconstruction of the intensity distribution in the incoherent imaging

II. Real optical systems and multi-point imaging quality criterion

RENATA NOWAK, IRENEUSZ WILK
Institute of Physics, Technical University of Wrocław, Wybrzeże Wyspiańskiego 27, 50-370 Wrocław, Poland.

In this paper the direct recovery method has been applied to the real (aberrated) optical systems. Its properties have been discussed so far as the influence of the sampling step, aberrations and the boundary sampling points on the reconstruction error is concerned. A new multi-point measure of imaging quality has been proposed being defined by the reconstruction errors for the actual systems as related to its diffraction-limited counterparts.

1. Introduction

In the previous paper [1] the results of numerical reconstruction of the intensity distribution by using the direct recovery method [2] have been presented for the case of diffraction-limited systems.

In this paper we show the results of applying the direct recovery method to the image intensity reconstruction for real telescopic, photographic and enlarging optical systems. Besides, an attempt has been made to define a new multi-point measure of the imaging system quality based on the concept of the reconstruction error given in [2]. In these respects the present paper is a direct continuation of the analysis given in [1].

Table 1. Parameters of the selected optical systems: f' — image focal length, a — field angle

Objective number	f' [mm]	f-number	a
I	99.15	4.5	3°
II	99.77	4.5	3°
III	103.26	4.5	15°
IV	98.4	3.5	3°
V	100.58	4.5	15°
VI	105.6	4.5	37°

The method and algorithms useful in numerical estimations of the reconstruction matrix elements as well as in the reconstruction of the image intensity distribution for the real optical systems have been discussed in paper [3].

* This work was carried on under the Research Project M. R. I.5.

The basic parameters of the concrete objectives used in our calculations are given in table 1. The responses of the three first telescopic systems may be found in [4], while the two next are characterized in details in [5]. In particular, the system VI is the enlarger AMAR objective (of PZO* make) of the focal length 105.6.

2. Numerical reconstruction of the image intensity distribution for some real optical systems

2.1. The effect of changes in sampling steps on the reconstruction process

The reconstruction is performed for the types of objectives mentioned in the *Introduction*. We assume the integrating element of radius $R_E = 0.0032$ mm and the sampling step d, from the interval $0.005 \text{ mm} \leqslant d \leqslant 0.008$ mm.

Generally, it has been stated by numerical analysis that, similarly as it was the case for diffraction-limited counterpart systems considered in [1], the values of the recovered intensities increase with the increase of the sampling steps. This time, however, some sporadic deviations from this rule may happen.

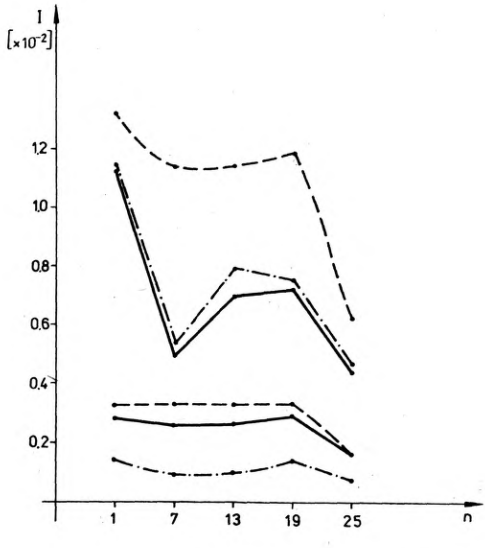

Fig. 1. Changes in the upper and lower bound intensity distributions as related to the sampling step for the system III (axial imaging): – – – – $d = 0.008$ mm, ——— $d = 0.0064$ mm, –.–.–. $d = 0.006$ mm

In the figure 1 the changes in upper and lower bound intensity distributions are shown for the optical system III and the sampling steps $d = 0.006$, 0.0064, and 0.008 mm (the results concern the points on the diagonal of the reconstructed image area which represent the sampling points Nos. 1, 7, 13, 19, and 25).

The reconstructed lower bound values of intensity distributions increase with the sampling step and the less the sampling steps ($d = 0.006$ and 0.0064 mm) the stronger this effect.

* Name of Polish Optical Works, in Warsaw.

In spite of the general tendency that the upper bound values of the reconstructed intensity distribution increase with the increasing sampling steps (fig. 1) the opposite situation is also observed, for instance, for $d = 0.006$ mm. The table 2 illustrates the changes in the intensity spread function of the system

Table 2. The changes in the intensity spread function (unnormed) for the system III (axial imaging)

r [mm]	0	0.001	0.003	0.005	0.006	0.007	0.0077
$\varphi(r)$ $[10^{-1}]$	1.701	0.682	0.184	0.141	0.172	0.162	0.108

III in the radial direction. It may be seen that for the distance $d \simeq 0.006$ mm there appears a samall maximum, which causes an unusual course of the changes in the reconstructed intensity distributions from fig. 1.

While, for the diffraction limited systems the inversion* of the upper and lower bound intensity distribution appeared only for great sampling steps and resulted from the diminished accuracy of the numerical estimation of the matrix elements, for the case of real systems the inversion may be additionally caused by the specific character of the intensity distribution within the aberration spot, especially in the boundary regions of the spread functions.

For instance, the inversion of the upper and lower bound intensity distributions for the telescopic system IV is observed for the majority of the sampling steps assumed. The changes in the intensity spread function of the system IV (tab. 3 and fig. 2) explain the reasons for the inversion of the extreme values of intensity.

From the table 3 it may be seen that the whole energy is concentrated practically within the region of radius $r \leqslant 0.01$ mm, while within the much larger region of radius $r \leqslant 0.025$ mm it increases only slightly. Therefore, for small sampling steps the sum of the energy contributions from the closest

Table 3. The changes in the intensity spread function (unnormed) for the system IV (axial imaging)

r [mm]	0	0.0025	0.005	0.01	0.0125	0.0175	0.002	0.0225
$\varphi(r)$ $[10^{-2}]$	2.82	2.72	1.23	0.11	0.058	0.047	0.01	0.026

neighbours in the case of the lower bound reconstruction may exceed that of energy contributions supplied by the respective neighbours in the case of the upper bound reconstruction. This is explained in fig. 2 which illustrates the

* In the case of intensity inversion at a given point the absolute value of the reconstructed upper bound intensity is less than that for lower bound intensity.

mutual positions of the integrating element and the intensity spread functions generated by two image points for the sampling step $d = 0.005$ mm.

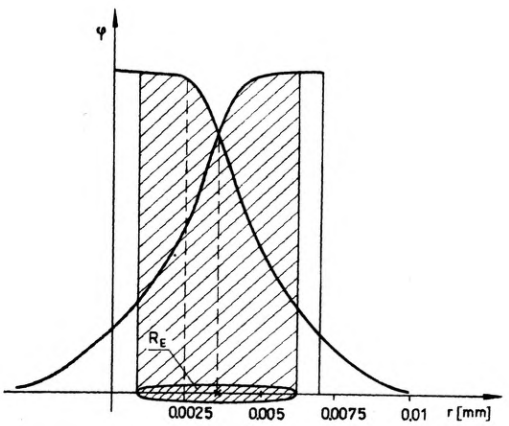

Fig. 2. Mutual position of the spread function for two image points and that of the integrating element for the case of upper bound reconstruction (sampling step $d = 0.005$ mm, integrating element of radius $R_E = 0.0032$ mm)

3. Normalization of the aberrational spread function

Usually for the real optical systems it is not difficult to find their diffraction-limited counterparts of the same f-number. In order to compare the image intensity distributions reconstructed for a real imaging system with those generated by the corresponding aberration free optical system it is necessary to normalize properly the aberrational spread function. For this purpose it is easy to notice that the quantity of energy contained within the domain of aberrational spread functions must be equal to that contained within the domain of the corresponding diffraction-limited spread function, i.e.

$$\int_P \varphi^{\text{diff}} ds = k \int_{P_1} \varphi^{\text{aberr}} ds, \tag{1}$$

where P, P_1 — the respective domains of the diffraction-limited and aberrational spread functions,

k — the normalizing factor.

Both the integrals in (1) have been evaluated numerically by the method of spot-diagrams [3], and hence the normalizing factor was estimated.

In the table 4 the quantities are given, which allow to find the diffraction-limited counterparts and the values of the respective normalizing factors, for the real objectives chosen to the reconstruction procedure. In the same table the conventional radii of the respective domains of the real and aberration-free spread functions φ^{aberr}, and φ^{diff} are compared.

Table 4. Basic parameters of the examplified real systems: D' – exit pupil diameter, S' – distance of the exit pupil from the image, k – normalizing factor, R_φ^{diff} – radius of the domain of the diffraction limited intensity spread function limited to the second minimum, R_φ^{aberr} – radius of the circle in the domain of the aberration spread function (axial imaging [3])

Objective number	D' [mm]	S' mm	S'/D'	k [$\times 10^2$]	R_φ^{diff} [mm]	R_φ^{aberr} [mm]
I	22.47	101.11	4.5	3.66	0.0058	0.0046
II	22.17	99.62	4.5	3.51	0.0058	0.0053
III	22.44	104.58	4.5	3.75	0.0058	0.0078
IV	31.77	111.22	3.5	0.58	0.0045	0.0353
V	23.9	107.64	4.5	4.07	0.0058	0.0240
VI	22.06	152.31	6.9	3.47	0.0089	0.0570

4. The effect of the aberrations on the reconstruction error

The most interesting is the comparison of the image intensity distributions reconstructed in the case of real optical systems with those recovered for the aberrationless optical systems; the reconstruction parameters d, R_E being the same. In the tables 5, 6 and 7 the extreme reconstructed image intensities are listed for different systems: (photographic) III, (telescopic) V, and (enlarging) VI. From the graphs of the respective transfer functions (fig. 3) it may be seen that these systems differ in aberration correction. It is easy to notice that the reconstruction error [1]:

$$\Delta I = |I^{\max} - I^{\min}| \tag{2}$$

becómes the smaller the lower the quality of the imaging system.

This point, surprising at the first sight, is in fact consistent with the physical intuition. To make it clear it suffies to notice that: the better the optical system the more detailed information may be transferred through this system, i.e. the more complex image structure to be sampled. If both the sampling system and the sampling procedure (sampling configuration and sampling steps) are fixed, and if there exists no prior-to-measurement information about the imaged object, then the resulting error must be greater.

On the other hand, the same result may be interpreted in another way, more suitable to discussion of the multiple-point measure of the imaging quality proposed below. Namely, it is obvious that having assumed the same sampling results for both the diffraction-limited and real systems the due changes in the

Table 5. Comparison of the extreme reconstructed image intensity distributions and the reconstruction errors for the system III (photographic) with its diffraction-limited counterparts (axial imaging)

Reconstruction for a diffraction-limited system, $N = 1:4.5$					Reconstruction for a real photographic system III				
Upper bound image density distribution $I^{max} \times 10^{-1}$					Upper bound image intensity distribution $I^{max} \times 10^{-1}$				
1.37	1.37	1.37	1.37	0.96	1.32	1.20	1.22	1.24	0.89
1.37	1.37	1.37	1.37	0.96	1.20	1.14	1.14	1.16	0.82
1.37	1.37	1.37	1.37	0.96	1.22	1.14	1.15	1.17	0.83
1.37	1.37	1.37	1.37	0.96	1.24	1.16	1.17	1.19	0.84
0.96	0.96	0.96	0.96	0.96	0.89	0.82	0.83	0.84	0.62
Lower bound image intensity distribution $I^{min} \times 10^{-1}$					Lower bound image intensity distribution $I^{min} \times 10^{-1}$				
0.014	0.014	0.014	0.014	0.010	0.33	0.33	0.33	0.33	0.23
0.014	0.014	0.014	0.014	0.010	0.33	0.33	0.33	0.33	0.23
0.014	0.014	0.014	0.014	0.010	0.33	0.33	0.33	0.33	0.23
0.014	0.014	0.014	0.014	0.010	0.33	0.33	0.33	0.33	0.23
0.010	0.010	0.010	0.010	0.007	0.23	0.23	0.23	0.23	0.16
Reconstruction error $\Delta I \times 10^{-1}$					Reconstruction error $\Delta I \times 10^{-1}$				
0.68	0.68	0.68	0.68	0.47	0.49	0.43	0.44	0.45	0.33
0.68	0.68	0.68	0.68	0.47	0.43	0.40	0.40	0.41	0.29
0.68	0.68	0.68	0.68	0.47	0.44	0.40	0.41	0.42	0.30
0.68	0.68	0.68	0.68	0.47	0.45	0.41	0.42	0.43	0.30
0.47	0.47	0.47	0.47	0.34	0.33	0.29	0.30	0.30	0.22

Table 6. Comparison of the extreme reconstructed image intensity distributions and the reconstruction errors for the system V (telescopic objective) with its diffraction-limited counterparts (axial imaging)

Reconstruction for a diffraction-limited system $N = 1:4.5$					Reconstruction for a real telescopic system V				
Upper bound image intensity distribution $I^{max} \times 10^{-1}$					Upper bound image intensity distribution $I^{max} \times 10^{-1}$				
1.37	1.37	1.37	1.37	0.96	0.79	0.73	0.74	0.75	0.54
1.37	1.37	1.37	1.37	0.96	0.73	0.69	0.69	0.70	0.50
1.37	1.37	1.37	1.37	0.96	0.74	0.69	0.69	0.71	0.50
1.37	1.37	1.37	1.37	0.96	0.75	0.70	0.71	0.72	0.51
0.96	0.96	0.96	0.96	0.68	0.54	0.50	0.50	0.51	0.37

Table 6 (continued)

Lower bound image intensity distribution $I^{min} \times 10^{-1}$					Lower bound image intensity distribution $I^{min} \times 10^{-1}$				
0.014	0.014	0.014	0.014	0.010	0.32	0.33	0.33	0.32	0.21
0.014	0.014	0.014	0.014	0.010	0.33	0.34	0.34	0.33	0.22
0.014	0.014	0.014	0.014	0.010	0.33	0.34	0.34	0.33	0.22
0.014	0.014	0.014	0.014	0.010	0.32	0.33	0.33	0.32	0.21
0.010	0.010	0.010	0.010	0.007	0.21	0.22	0.22	0.21	0.14
Reconstruction error $\Delta I \times 10^{-1}$					Reconstruction error $\Delta I \times 10^{-1}$				
0.68	0.68	0.68	0.68	0.47	0.24	0.20	0.20	0.22	0.16
0.68	0.68	0.68	0.68	0.47	0.20	0.17	0.17	0.19	0.14
0.68	0.68	0.68	0.68	0.47	0.20	0.20	0.17	0.19	0.14
0.68	0.68	0.68	0.68	0.47	0.22	0.19	0.19	0.20	0.15
0.47	0.47	0.47	0.47	0.34	0.16	0.14	0.14	0.15	0.11

Table 7. Comparison of the extreme reconstructed image intensity distributions and the reconstruction errors for the system VI (enlarger) with its diffraction-limited counterpart (axial imaging)

Reconstruction for a diffraction-limited system, $N = 1:4.5$					Reconstruction for a real enlarger system VI				
Upper bound image intensity distribution $I^{max} \times 10^{-1}$					Upper bound image intensity distribution $I^{max} \times 10^{-1}$				
0.57	0.61	0.61	0.57	0.44	0.21	0.23	0.24	0.22	0.18
0.61	0.66	0.66	0.61	0.44	0.23	0.26	0.27	0.23	0.19
0.61	0.66	0.66	0.61	0.44	0.24	0.27	0.27	0.25	0.19
0.57	0.61	0.61	0.57	0.44	0.22	0.24	0.25	0.23	0.18
0.44	0.44	0.44	0.44	0.37	0.18	0.19	0.19	0.18	0.16
Lower bound image intensity distribution $I^{min} \times 10^{-1}$					Lower bound image intensity distribution $I^{min} \times 10^{-1}$				
0.11	0.11	0.11	0.11	0.08	0.39	0.41	0.41	0.39	0.27
0.11	0.12	0.12	0.11	0.08	0.41	0.41	0.41	0.41	0.28
0.11	0.12	0.12	0.11	0.08	0.41	0.41	0.41	0.41	0.28
0.11	0.11	0.11	0.11	0.08	0.39	0.41	0.41	0.39	0.27
0.08	0.08	0.08	0.08	0.07	0.27	0.28	0.28	0.27	0.22
Reconstruction error $\Delta I \times 10^{-1}$					Reconstruction error $\Delta I \times 10^{-1}$				
0.23	0.25	0.25	0.23	0.18	0.09	0.09	0.08	0.08	0.04
0.25	0.27	0.27	0.25	0.18	0.09	0.07	0.07	0.09	0.04
0.25	0.25	0.27	0.25	0.18	0.08	0.07	0.07	0.08	0.04
0.23	0.25	0.25	0.23	0.18	0.08	0.08	0.08	0.08	0.04
0.18	0.18	0.18	0.18	0.15	00.4	0.04	0.04	0.04	0.03

reconstruction error may be attributed to the aberrations of the optical system (see tables 5, 6, 7, and fig. 3), and, consequently, used to define a multi-point measure of the imaging quality (see Section *Multi-point measure of imaging quality*).

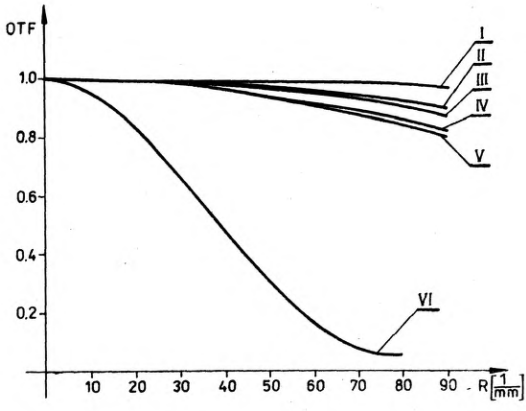

Fig. 3. Monochromatic optical transfer function (V). Axial imaging

5. The influence of the boundary sampling points on the reconstruction process for the real optical systems

In the reconstruction examples, discussed earlier for the real imaging systems, the sampling steps d ranged within the interval $0.005 \leqslant d \leqslant 0.008$ mm.

As it should be expected, in this case, the least admissible sampling step is much greater than that for the respective analogous diffraction limited systems; the least admissible sampling step being assumed to be the distance between the two neighbour sampling points for which the solutions C_i of the reconstruction equations:

$$y(p_k q_k) = \sum_{i=1}^{N} C_i \int \varphi^{\mathrm{I}}(\alpha_i - p, \beta_i - q) \int \varphi^{\mathrm{II}}[u-(p-p_k),\ v-(q-q_k)]$$
$$du\,dv\,dp\,dq, \quad k = 1, \ldots, n \tag{3}$$

are still non-negative. Here, $y(p_k, q_k)$ — the result of sampling in the $(p_k q_k)$-point, φ^{I}, φ^{II} — the spread functions of the imaging and measuring systems, respectively.

The following discussion aims at determining certain properties of the numerically simulated reconstruction procedure which are of special importance for defining and using of the multi-point measure of the optical system quality.

To facilitate the future comparison of the numerical reconstruction for different aberrated systems it is necessary to normalize some parameters of the reconstruction procedure, for example, the sampling step d. The decision how to normalize the sampling is by no means simple, as it turns to be correlated to the others reconstruction parameters, for instance, to the sampling point values.

It has been found numerically that the least sampling step, common to all the aberrated systems considered above, is $d = 0.005$ mm. However, this value may suffer from considerable fluctuations depending upon the postulated measurement results at the boundary sampling points of the sampled region.

It has been stated that an increase of the postulated sampling results at the boundary points may cause a considerable increase in the least admissible sampling step. For instance, for the telescopic system V an increase of the postulated sampling values at the boundary sampling points by 20 % causes the increase of the least admissible sampling step from $d = 0.005$ to $d = 0.008$ mm, while for telescope system IV the respective increase reached only the value $d = 0.0064$. This difference may be explained by the fact that the system IV is better corrected than the system V.

The considered numerical examples indicate that the aberration-free systems show much greater tolerance for the changes in the postulated sampling results at the boundary points than the real system. For instance, for the diffraction-limited counterparts of the systems IV and V there exist solutions of the reconstruction procedure for many sampling steps and the measurement results which would not be unacceptable for the true aberrated system. Table 8 illustrates the influence of the changes in the sampling results at the boundary points on the image intensity reconstruction at the image points. The differences between the reconstructed intensity values (differing in the boundary points) for the case of the real system V and its diffraction-limited counterpart were calculated and presented in table 8, for the sampling result distributions of types I and II (parts A and B).

Additionally, the influence of the same changes in the sampling results at the boundary points on the extreme intensity distributions has been pointed out for the telescope system IV, which is slightly better corrected than the system V (tab. 8, part C).

It may be seen (tab. 8, part A) that for the aberration-free systems there exists only slight influence of the change in the intensity measurement results at the boundary points in the case of the upper bound reconstruction (and it affects only the boundary points), which, however, is much more distinct in the lower bound reconstruction. It has been found that the differences between the reconstructed intensities evoked by the change in the sampling point values at the border decrease with the increase of the sampling step.

A similar tendency exists also for the aberrated system. Here, the influence of the boundary points both in the upper bound and lower bound reconstructed intensity distributions is much greater than in the analogous aberration-free system (tab. 8, part B). For instance, in the case of the system V it may be

Table 8. Influence of the change in the sampling point values at boundary points on the reconstruction of the image intensity distribution in the remainder points. The reconstruction being made for $d = 0.005$ mm and $R_E = 0.0032$ mm. $I_{\mathrm{I}}^{\max}$, $I_{\mathrm{I}}^{\min}$, $I_{\mathrm{II}}^{\max}$, $I_{\mathrm{II}}^{\min}$ – the extreme image intensity distributions reconstructed for the I and II sampling point configurations

		Configuration I					Configuration II				
		1	1	1	1	0.7	1	1	1	1	0.5
Postulated		1	1	1	1	0.7	1	1	1	1	0.5
sampling		1	1	1	1	0.7	1	1	1	1	0.5
result		1	1	1	1	0.7	1	1	1	1	0.5
		0.7	0.7	0.7	0.7	0.5	0.5	0.5	0.5	0.5	0.3
		$\Delta I^{\max} = I_{\mathrm{II}}^{\max} - I_{\mathrm{I}}^{\max}$					$\Delta I^{\min} = I_{\mathrm{II}}^{\min} - I_{\mathrm{I}}^{\min}$				
A	Diffraction-limited system $n = 1:4.5$	0	0	0	0.01	0.01	0.02	0.02	0.02		
		0	0	0	0.01	0.02	0.03	0.03	0.02		
		0	0	0	0.01	0.02	0.03	0.03	0.02		
		0.01	0.01	0.01	0.02	0.02	0.02	0.02	0.04		
		$\Delta I^{\max} = I_{\mathrm{II}}^{\max} - I_{\mathrm{I}}^{\max}$					$\Delta I^{\min} = I_{\mathrm{II}}^{\min} - I_{\mathrm{I}}^{\min}$				
B	Telescopic system V $N = 1:4.5$	0.01	0.01	0.06	0.06	No solutions for					
		0.01	0.04	0.02	0.07	II configuration					
		0.06	0.02	0.06	0.07	of measuring points					
		0.04	0.07	0.07	0.03						
		$\Delta I^{\max} = I_{\mathrm{II}}^{\max} - I_{\mathrm{I}}^{\max}$					$\Delta I^{\min} = I_{\mathrm{II}}^{\min} - I_{\mathrm{I}}^{\min}$				
C	Telescopic system VI $N = 1:3.5$	0.01	0.01	0.01	0.02	0.03	0.14	0.14	0.02		
		0.01	0.01	0.01	0.03	0.14	0.07	0.07	0.14		
		0.01	0.01	0.01	0.04	0.14	0.07	0.07	0.14		
		0.02	0.03	0.04	0.05	0.03	0.14	0.14	0.02		

seen that the change in the postulated measurement results at the boundary points makes sometimes the upper bound reconstruction impossible. The differences in the upper bound intensity distributions for the system V are distinctly greater than those for the aberrated systems appearing in the same situation even for the lower bound reconstruction.

By comparing the differences in the reconstructed intensities for the systems V and IV (tab. 8, part B and C) it may be seen that the sensitivity of the reconstructing procedure to a change in the measurement results at the boundary sampling points (the values attributed to the other points being unchanged) depends essentially upon the system correction. The poorer system shows much less tolerance for the admissible changes in the value of the sampling results at the boundary points.

This property shows some difficulties which may occur when simulating the reconstructing experiments, for instance, for the purpose of constructing the multi-point measures of the imaging quality*.

6. Multi-point measure of imaging quality

The construction of a measure or a criterion of the imaging quality which would be applicable in practice is still one of the most important problems of the contemporary theory of optical imaging. There exist a number of measures or criteria proposed so far by many authors and based on different concepts. Just to name some examples we may distinguish: single-point criterion (represented, for instance, by Strehl definition or Maréchal criterion), two-point criterion or measure (like that of Rayleigh), continuous type measures (like Linfoot fidelity defect or relative structural content). There exist also some criteria based on statistical approach and information theory. The main problems seems to lie in construction of such criterion or measure that would be universal enough to be used in wide variety of very different problems. The multi-point recovery measure proposed below seems to meet the requirement of higher than usual universality at reasonable costs of computing time and therefore may be useful for optical system designer.

Let us accept the expression

$$M = \frac{\sum_{i=1}^{N} |\Delta I_i|^{\text{aberr}}}{\sum_{i=1}^{N} |\Delta I_i|^{\text{diff}}} \tag{4}$$

as a multi-point measure of the imaging quality within the recovered region of the image. Here $|\Delta I_i|^{\text{aberr}}$ is the absolute value of the reconstruction error for the real aberrated optical system at the i-th sampling point, $|\Delta I_i|^{\text{diff}}$ is the absolute value of the reconstruction error for its diffraction-limited counterpart at the same sampling point.

There are three features distinguishing this measure from the others: firstly, it relates the actual optical system to that of ideal (diffraction-limited) counterpart, secondly, it encounters the mutual influence of the neighbouring object points on the respective image points, thirdly, it takes accont of the specificity of the measuring (observing) system used in assessing the object quality which makes the assessment more realistic.

As may be easily noticed the multi-point measure satisfies the inequality

$$0 \leqslant M \leqslant 1. \tag{5}$$

* It is quite obvious that such difficulties never appear for real reconstruction procedure based on real measurement results. In these situation the direct recovery method always works.

The better the correction of the estimated optical system the greater reconstruction errors $|\Delta I_i|^{aberr}$, $i = 1, \ldots N$ and, consequently, the greater value of the proposed multi-point measure. In the table 9 the calculated multi-point reconstruction measures of imaging quality for some chosen optical systems are given as they depend upon the sampling steps for the sampling restricted to the one-dimensional case.

Table 9. Dependence of the multi-point reconstruction measure of imaging quality upon the sampling step (d)

Objective number	$d = 0.005$ mm	$d = 0.006$ mm	$d = 0.0064$ mm	$d = 0.008$ mm
I	0.8500	0.8800	0.9800	*
II	0.7900	0.8080	0.7240	0.9500
III	0.6300	0.6150	0.4400	0.6700
IV	0.3800	0.3200	0.3900	0.5800
V	0.3100	0.2450	0.0980	0.2940
VI	0.0034	0.0031	0.0025	0.0039

* – absence of the lower bound matrix (due to too great sampling step)

From the calculated examples it may be seen that the value of the multi-point measure depends on the sampling step. This means that a comparison of the quality of different optical systems or the consecutive version of the same system obtained subsequently in the designing procedure may be done only for fixed sampling steps. As expected the value of the multi-point reconstruction error decreases for systems of worse correction which may be noticed by comparing the table 9 with fig. 3, in which the curves of monochromatic modulation transfer function is presented for the systems I–IV for the axial imaging.

The said dependence of the multi-point measure on the sampling step is only one of three dependences of this kind. The other two are: dependence on the sampling configuration and dependence on the used measuring (observation) system.

These three dependences make the multi-point measure flexible and easily adjustable to the concrete tasks to be fulfilled by the designing optical system (including the detecting stage).

7. Concluding remarks

In this paper some general properties of the direct recovery procedure have been discussed for real (aberrated) systems and illustrated by numerical examples. In particular, the effect of changing the sampling step on the recovery procedure was considered. It was followed by the discussion of the correlation between the reconstruction error and the aberrations of the optical system under test which preceded by a normalizing procedure for aberrational spread function

to enable the due comparisons with the respective ideal diffraction limited case.

The results of these considerations were employed to define a new multi-point measure of the imaging quality of optical systems. This measure has been calculated for selected types of optical systems (like those of telescopes, enlargers and photographic cameras). It has been shown that the proposed measure proved to be very sensitive.

The calculations have been restricted to the axial region, since in this case it was possible to choose such a priori sampling results, which assure simultaneous solution of the upper and lower bound reconstruction equations under the additional condition of positivity of the reconstruction weights C_i.

The suggested multi-point measure seems to offer some additional advantages as compared to the single- and two-point measures. In particular:

i) it allows to take account of the mutual influence of many neighbouring points in the image on the measuring results which creates the situation closer to that occurring in the real imaging procedure ended by a detection stage,

ii) it takes account of the specificity of both the measurement (observation) system and the way of performing the measurement (observation) so far as the sampling configuration and sampling step are concerned, [6],

iii) it offers a possibility of including also the prior information (independent of the measurement results) about the object [6] into considerations as an essential determinant of imaging quality measure,

iv) it may be generalized to include the case of partially coherent imaging which would allow to determine the influence of the partial coherence on the quality of the imaging systems [6].

Unfortunately, the inclusion of the last two points in the reconstruction procedure results in a considerable increase of calculation complexity.

Finally, it is worth noting that both the reconstruction procedure and the resulting multi-point measure is especially suitable in the optical systems, at the exit of which a sampling procedure is applied with the help of a "point" detector with automatic data processing.

References

[1] Nowak R., Wilk I., Optica Applicata **X** (1980), 351.
[2] Wilk I., Pr. nauk. Inst. Fizyki PWr., No. 4, 1970, p. 3.
[3] Nowak R., Karaś M., Optica Applicata **V** (1975), 27.
[4] Nowak R., Nowak J., Report No. 183, Institute of Physics, Technical University of Wrocław, Wrocław 1974.
[5] Nowak J., Doctor's Thesis, Institute of Physics, Technical University of Wrocław, Wrocław 1972.
[6] Wilk I., Optica Applicata **II** (1973), 3.

Received November 21, 1979
in revised form August 26, 1980

Численная реконструкция распределения интенсивности в некогерентном отображении

II. Реальные оптические системы и многоточечный критерий качества отображения

Обсуждены результаты численных расчётов распределений интенсивностей в изображении полученных методом непосредственной реконструкции по отношению к реальным оптическим системам. Доказано, что процедура непосредственной реконструкции может служить для определения новой, многоточечной меры качества. Для избранных типов оптических (фотографических, телескопических и увеличительных) систем была рассчитана, в случае отображения на оси, предлагаемая многоточечная мера для различных шагов пробирования. На основе сопоставления с оптической функцией переноса констраста можно отметить, что предлагаемая мера является пригодной для оценки коррекции оптических систем и обладает высокой чувствительностью.